Supporting Online Material for

Quaternary coral reef refugia preserved fish diversity

L. Pellissier, F. Leprieur, V. Parravicini, P. Cowman, M. Kulbicki, G. Litsios, S. Olesen, M. S. Wisz, D. R. Bellwood, D. Mouillot

Correspondance to:
D. Mouillot
UMR 5119 ECOSYM
Université Montpellier 2
Place Eugène Bataillon,
34095 Montpellier Cedex 5
France
Email: david.mouillot@univ-montp2.fr
Fax: +33 4 67 14 37 19

Materials and methods

Present and past ocean temperature data

Sea surface temperature (SST) reconstructed for the historic period prior to the recent global increase in temperature in the last 50 years (Fig. S1). Here, we exploited a global ocean hindcast simulation covering the pre-warming decades of interest 1948-1968. The model consist of the coupled ocean-sea ice module NEMO-LIM in the configuration embedded in the EC-Earth climate model (34) with a basic resolution of 1°x1° and a meridional equatorial refinement to 1/3°. Initially, the model state is equilibrated during a multi-centennial spin-up simulation. In the final reconstruction we apply historic 6-hourly atmospheric forcing from NCEP/NCAR reanalysis project to constrain the model and sea surface temperature in particular (35). Quaternary sea surface temperature and sea level were inferred from sediment

cores. Knowledge of sea levels and sea surface temperature for past time periods relies on proxy indicators contained within calcareous remains of marine foraminifera (17, 18). Sediment cores record the chemical signatures of the water in which those organisms lived, which provides information on past sea surface temperature and sea level (Fig. S1) (17, 18). Foraminifera records in sediment cores are available up to the last five million years. We collected 27 time series providing information on past sea surface temperature and three of sea level covering parts of the last three million years and distributed across the tropical and subtropical seas of the globe (17-18, 35-50). Data were downloaded from ftp://ftp.ncdc.noaa.gov/pub/data/paleo. We computed differences between the core and 1948-1968 sea surface temperature for each core location to obtain anomalies. We tested for the temporal correlation between cores (Fig. S2). Ideally, geostatistical interpolations of anomalies should be used to capture local trends, but since the number of spatial replicates is insufficient for older time periods, we computed an average of anomalies across all cores with available data for each 1000 years. We applied anomalies on current sea surface temperature and a global digital elevation maps at a resolution of 30 arc-second to build approximate temperature and sea level maps of the last three million years with 1000 years interval. We acknowledge that applying sea surface temperature anomalies to a map depicting current hydrography is unlikely to fully represent the spatio-temporal variation in climate. During cold periods regional ocean currents were probably different from how they are today impacting local sea surface temperature. However, the effect of shifts in ocean circulation across time is unlikely to have a major effect on our reconstructions as we considered tropical seas which tend to display spatially more homogeneous yearly average sea surface temperatures (Fig. S1).

Coral reef habitat suitability model

Coral reefs are broadly recognized as being limited to warm, clear, shallow, and fully saline waters, which allows us to calibrate a simple environmental envelope model (8). Both empirical (6) and experimental (51, 52) evidence indicate that, on average, coral reefs thrive best and are globally distributed above a temperature of 25°C. Corals can tolerate temperatures lower than 25° (53), but reef formation is less likely in those suboptimal conditions. We further tested whether the probability of occurrence of coral reef dropped beyond a threshold of 25°C using a distribution model approach (54). We related coral reef occurrences (from www.reefbase.org) to current yearly average sea surface temperature. We used 10'000 pseudo-absences distributed randomly across the seas of the globe (55). We ran a generalized linear model (GLM) with a binomial distribution and a logistic link function and plotted the response curve. Confirming previous studies, we found a strong decrease of the probability of occurrence of coral reef below a threshold of 25°C indicating an optimum for the formation of coral reef above 25°C (Fig. S11). Coral reefs are also constrained by high temperature with mortality recorded at temperatures above 32°C (56), but the exact high temperature threshold is not precisely known given that coral reefs have a realized distribution spanning the warmest waters on the globe. As a consequence, we focused on coral reef response to cold temperature events, while acknowledging that warm temperature during interglacial periods may also have had an effect on reef distribution (6, 57, 58). In addition, tropical coral reefs do not occur below a depth of -75 meters because of light limitation (6). The two considered environmental variables and associated thresholds, average SST >25°C and sea depth >-75m, define an environmental envelope that has the advantage of relying on information available for the Quaternary as described in the previous section. We validated our model using occurrences and pseudo-absences distributed across the globe. To assess the accuracy of our environmental envelope model, we used the Kappa metric as well

as the percentage of cases correctly classified (59). The use of climatic factors to calibrate the environmental envelope of coral species was already successfully used in a previous study (60). This envelope was used to define for each time step the distribution of coral reef at 1/3° resolution combined with past sea surface temperature and sea level maps.

We assessed the robustness of our envelope model for coral reefs based on core-inferred sea surface temperature and sea level with two supplementary analyses. First, sea surface salinity which was not accounted for in the model described above may also impacts coral reef establishment and distribution across the globe (6), but the effect of salinity is likely to be predominantly local. To test this, we reconstructed current sea surface salinity using the same hydrographic model as for sea surface temperature. We ran a GLM relating coral reef occurrences and pseudo-absences using both sea surface temperature and sea surface salinity and projected it for the current time period. We found a strong agreement between the model which included only sea surface temperature or both sea surface temperature and salinity, with only small differences at the mouth of the Amazon River, in the Bay of Bengal or in the Persian Gulf (Fig. S3). At the scale and resolution considered in our study and provided by the hydrographic model, sea surface salinity does not strongly limit coral reef distributions. Second, we projected the coral reef habitat model to the last glacial maximum using the most recent sea surface temperature anomaly reconstruction (61) and sea surface salinity (62) for that period. We compared our core inferred coral reef habitat surface per cell of 5°x5° during the last glacial maximum (average between the time periods from -19 to -23 Ky as considered in [61]) to this reconstruction and we found a very good agreement (Pearson's correlation=0.9) (Fig. S12, S13).

Past coral reef area and isolation from refugia

To compute past coral reef area for each time step, we aggregated the paleo-distribution of coral reefs to 5x5° resolution to match the spatial resolution of biodiversity data and computed the sum to obtain the total reef area per 5x5° cell. To summarize this information into a unique variable representing past reef surfaces, we estimate the average past reef area for the time periods when SST was below the 10^{th} percentile of all time periods.

We computed the total distance between each pixel and those with suitable reef conditions every millennium across three million years. For each time-step (every 1000 years) every time a given cell becomes suitable for coral reef in the time frame (t+1), we added the minimum sea distance from the closest cell suitable at time t. This distance accounted for the shape of land masses and was computed using the gdistance package (63) in the R software (64). We thus obtained the sum of distances needed to colonize a given cell across the entire period of climatic oscillations. Finally, we standardize this value by dividing by the number of time steps each cell was suitable during the three million years. This yielded a standardized distance required to recolonize a given cell from the nearest refugia through the last three million years after repeated phases of unsuitability. This approach was chosen because the effect of climate change on biodiversity is likely to be the cumulative result of climatic oscillations that varied in amplitude and shaped connectivity among reef habitats that varied through time.

Habitat fragmentation through time

In order to test for the effects of fragmentation of coral reef habitat on fish diversity patterns through time, we computed a habitat fragmentation index for each time step of 1000 year over the Indo-Pacific. For each time step, we cropped the coral reef distribution map to the Indo-

Pacific and computed an index of fragmentation of coral reef patches for this region. We used the landscape division index that reflects the probability that two randomly chosen pixels in the landscape are not situated in the same patch. To compute this index, we used the ClassStat function in the SDMTools package (65) in the R software (64). We related the habitat fragmentation index during the last three million years to time using a bivariate linear regression model. We also related the habitat fragmentation index to the SST anomaly (between the contemporary period 1948-1968 and each time step of 1000 year across three million years) to test whether stronger fragmentation occurred during colder time periods. We also compared the distribution of coral reef refugia to the expert-based ecoregions defined based on faunal composition (66).

Reef fishes distribution database

We obtained information on presence/absence of reef fish at 169 locations worldwide examining almost 500 references and extracting information from published works, regional checklists, monographs on specific families or genera, and reports (5). To increase the homogeneity of information among species lists, we focused our analysis on shallow water species. Overall, we obtained information on the distribution of 6316 reef fishes. As lists of each of the 169 locations are unlikely to have complete lists of the species that occur there, we constructed extent of occurrence map for each species, defined as the convex hull polygon of the locations where each species was present. Extent of occurrence maps included multiple polygons when clear range discontinuities exist. For this reason, each polygon was visually checked and reviewed by the authors according to their knowledge of reef fish species distributions. In the cases that discontinuities were detected, the initial convex hull was divided into multiple polygons to avoid disjointed distributions being merged (67). Species

composition was then extracted from a grid of 5°×5°, corresponding to approximately 555×555 km at the Equator. The grain size of the grid of 5°×5° was chosen because it represents a good compromise between the desired resolution and the geographical density of information.

We excluded from our analyses all cells containing land or those that did not contain coral reef or coastal habitat for shallow water species. Coastal habitat was defined as the ocean portion between 0m and 75m depth. Bathymetric data were obtained from the SRTM30_PLUS bathymetry (Shuttle Radar Topography Mission, available at: (http://topex.ucsd.edu/WWW_html/srtm30_plus.html) while information on the distribution of coral reefs was obtained from available information based on the Coral Reef Millennium Census project (68) and downloadable at: http://data.unep-wcmc.org. We removed cells with more than 90% of the surface is land. We additionally excluded those cells corresponding to areas were we had an original gap of information. These include the cells corresponding to the Gulf of Mexico, the estuary of the Amazon River and a few cells in the NW part of Australia.

Additional predictor variables

Current coral reef area has been shown to be a major driver of the diversity of coral reef fishes (5), as the greater the habitat area, the higher the number of species that can be maintained (68). We therefore estimated the total coral reef area (km^2) for each grid cell based on data obtained from the Coral Reef Millennium Census project (69). In order to account for the potential effect of current isolation of coral reef habitats, a measure of isolation was calculated based on connectivity among coral reef habitats. Connectivity was defined as the relative proximity of each reef patch to patches of reef fish habitat (defined below). Current connectivity estimates were calculated using a nearest neighbor approach, which is typically

employed in ecological research (70). In particular, using a Behrmann projection, the world was divided into cells (200 x 200 km at the equator) from which only cells containing reef fish habitat (i.e. coast or coral reef) were retained. These cells represent habitat patches and for each location we characterized current isolation of coral reef habitats by computing the inverse of the mean distance from a given pixel to the 10 nearest patches. We arbitrarily used 10 nearest neighbors instead of 1 in order to limit the strong dependency of the variable to a single neighbor, which may not always be highly connected to the most proximate reefs because of current flows. Energy availability is expected to influence the total number of species that can to co-exist (71). Even if sea surface temperature was previously shown to be of marginal importance in explaining tropical reef fish diversity (72), we used the current yearly average sea surface temperature SST as a proxy for energy availability.

Statistical analyses

Species richness patterns

First, we assessed the relationship between each of our historical (past coral reef area, isolation from refugia) and contemporary (current mean sea surface temperature, current coral reef area and current isolation) variables and reef fish species richness using a bivariate linear regression model. Subsequently, we ran a multiple ordinary least squares regression (OLS) model that includes all predictor variables. We used the coefficient of determination (R^2) to quantify the proportion of variation in species richness explained by the bivariate linear regressions and OLS models. OLS models may leave a variable degree of spatial autocorrelation in the residuals, which may bias parameter estimates and affect their statistical significance (73). We therefore compared the parameter estimates based on OLS to those obtained using a simultaneous autoregressive (SAR) model (74). A SAR model adjusts for

spatial autocorrelation by incorporating a spatially dependent error term. We used a spatial weight matrix with neighbourhoods defined as all cells within 800 km of the focal cell, and applied a Moran's I global test to determine whether residual autocorrelation persisted in the SAR models. We used a range of distances (i.e. 800, 1000, 1500 and 2000 km) to define the neighbourhood of each grid cell and preliminary analyses showed that only a distance of 800 km allowed removing spatial autocorrelation in model residuals. To account for potential non-linear associations between fish richness and the predictor variables, we tested the quadratic term of each predictor variable in the bivariate linear regression, OLS and SAR models. The current coral reef area variable was log-transformed prior analyses, because this variable showed a power relationship with species richness, better fitted with a log transformation than the addition of a quadratic term. This log transformation approach was used in previous studies analysing the effect of current coral reef area on reef fish richness (69).

Based on the full OLS and SAR models, information theoretic-based model selection was undertaken by comparing all competing models including all possible combinations of contemporary and historical variables. To do so, we used the Akaike information criterion (AIC) to quantify the support for each model (75). The selection of the minimum adequate model (MAM) was based on the lowest AIC value. From all subset models, we calculated the Akaike weight (w) that can be interpreted as the probability that a specific model is the best (74). We then estimated the relative importance of each predictor in explaining reef fish species richness by summing Akaike weight values across all models that include the predictor variable (75, 76). These summed Akaike weights (W_{AIC}) range from 0 to 1, hence providing a means for ranking the predictor variables in terms of information content (15). These analyses were performed using R (64) and the package "MuMIn" (77).

Finally, we employed a variance partitioning analysis (78) to quantify the relative importance of historical vs. contemporary variables in explaining species richness variation. This analysis

decomposes the variation in species richness (i.e. the R^2 of an OLS model) into three sources of variation by means of partial regressions (79): (i) variation due to the independent effect of historical variables, (ii) variation due to the independent effect of contemporary variables, and (iii) variation due to the combined effect of historical and contemporary variables.

We also tested the null hypothesis of no change of slope (Davies's test for difference-in-slope) to identify potential segment breakpoints in the regression models linking fish richness to the isolation from Quaternary refugia for each family (Figs. 2, B-D; S8). We detected nonlinear relationships with significant breaking points for the three relationships (P<0.0001) using the package "segmented" (80) implemented in R (64).

Species age patterns

For the analyses involving species age, we used the dated phylogenies of three families (Labridae, Chaetodontidae, Pomacentridae) published in (4). Species age was defined as the time of the most recent split with a sister species based on genetic differentiation. We first tested for the effect of isolation from refugia on the richness of young species (<3mia) using R^2 computed from a bivariate linear regression model. A SAR model accounting for spatial autocorrelation in model residuals was further used for parameter estimations. We then applied a similar methodology to test for the effect of isolation from refugia on the range of species age within species assemblages. To do so, we calculated the difference between the 95^{th} and 5^{th} percentiles of species age range for each grid cell. Because species richness is correlated with isolation from refugia and richer assemblages may have a larger range of species age due to a sampling effect, we compared the relationship between the observed range of species age and isolation from refugia to 999 relationships where the range of species age was calculated after having randomized species labels on the phylogeny (Fig. S10). While

the phylogenies of the three families studied are not fully resolved, spatial patterns of species richness based on the species included in the phylogenies are highly congruent with those based on the total number species (Fig. S14).

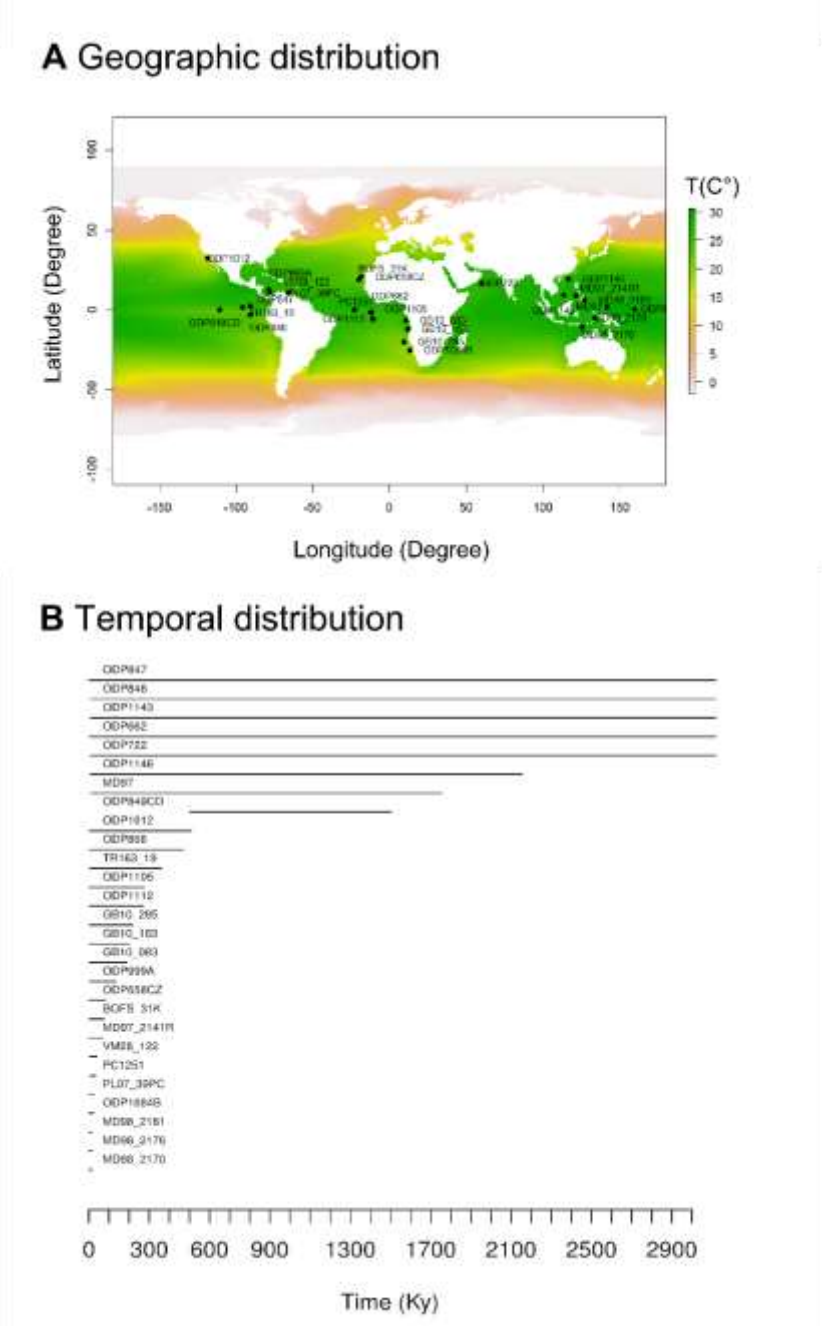

Fig. S1 – (A) Map of the distribution of the 27 sediment cores. The colour layer represents yearly average sea surface temperature inferred for the period 1948-1968 at a resolution of 0.5x0.5°. (B) Temporal coverage of the 27 sediment cores.

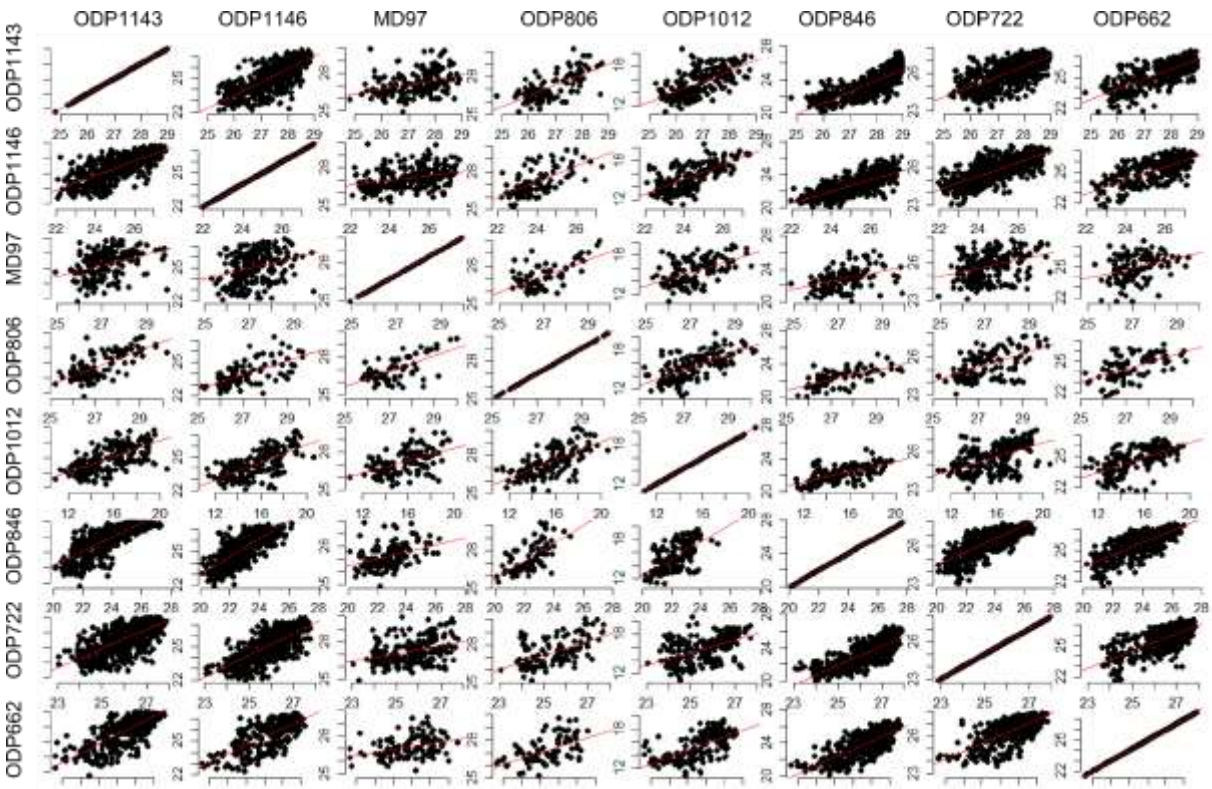

Fig. S2 – Relationships between sea surface temperatures estimated from the eight sediment cores with the longest coverage across time. Shown in order are "ODP1143", "ODP1146", "MD97", "ODP806", "ODP1012", "ODP846", "ODP722", "ODP662".

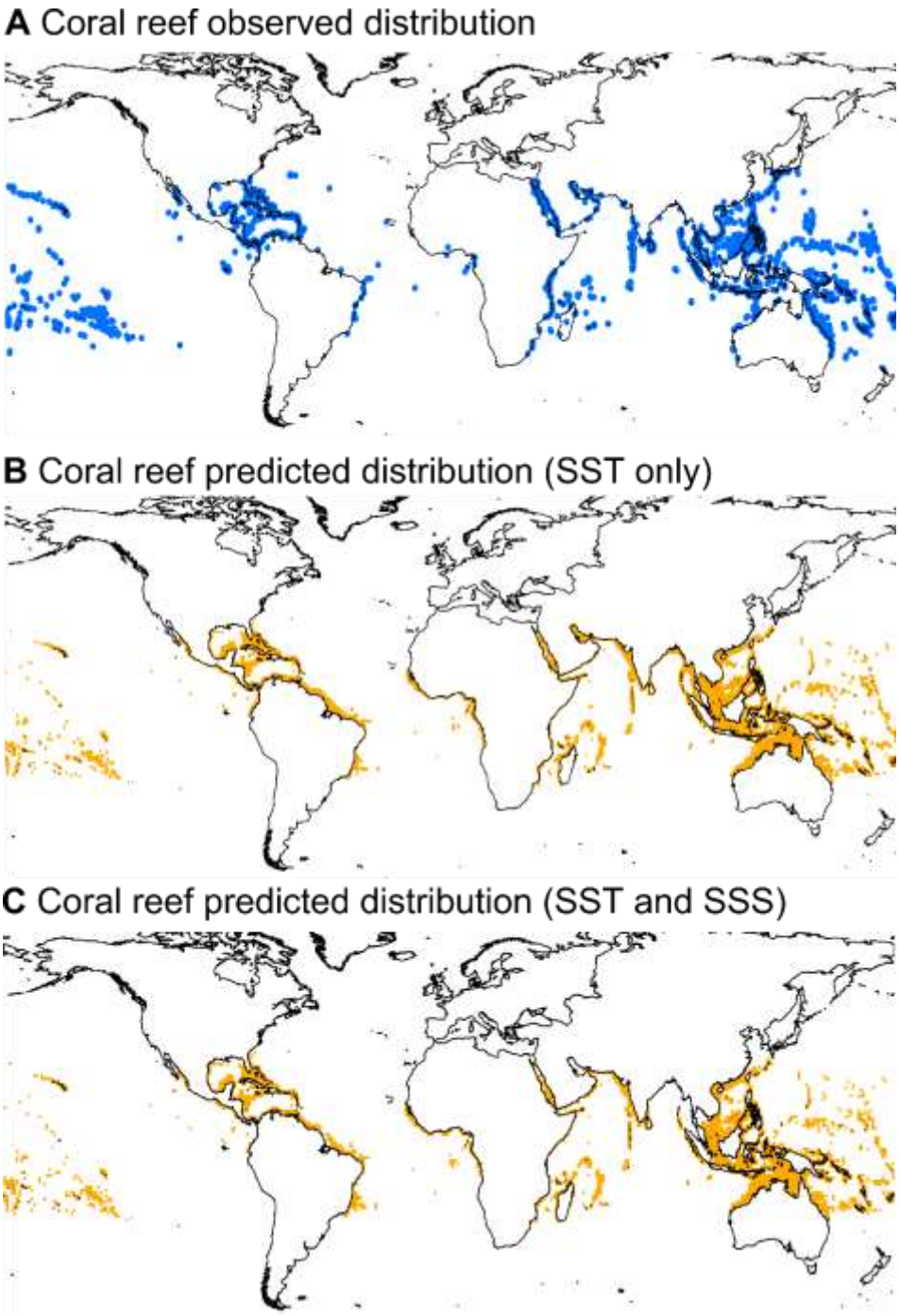

Fig. S3 – Maps of observed occurrence of coral reef habitat (www.reefbase.org) (A) and of current suitable habitat for coral reefs predicted by the boundaries of sea level and yearly average sea surface temperature (B). Average sea surface temperature and depth accurately predict accurately current global distribution of coral reef habitat (Kappa = 0.95 and 95% of correct classification). Also shown is the distribution of coral reefs predicted using both sea surface temperature and sea surface salinity (C). The two models present only small differences such as at the mouth of the Amazon River, in the Bay of Bengal or in the Persian Gulf.

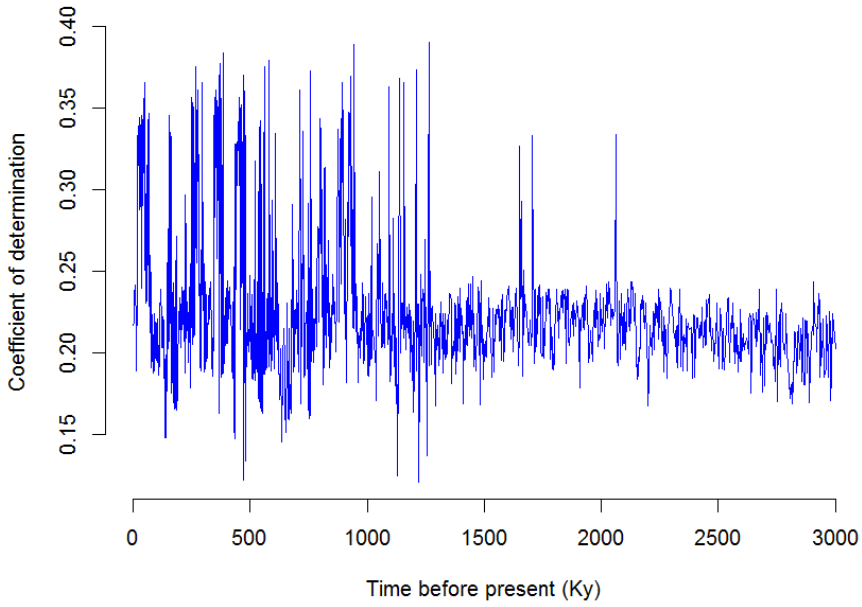

Fig. S4 – Relationship between the time before present (Ky) and the coefficient of determination (R^2) of the bivariate regression between reef fish richness and past coral reef area (log-transformed) obtained from the past reef reconstruction for each time step of 1000 year during the last three million years. Coefficient of determination was highest during past periods with lower SST and sea level stands impacting coral reef area with the maximum R^2=0.39 at -1.264 Ma.

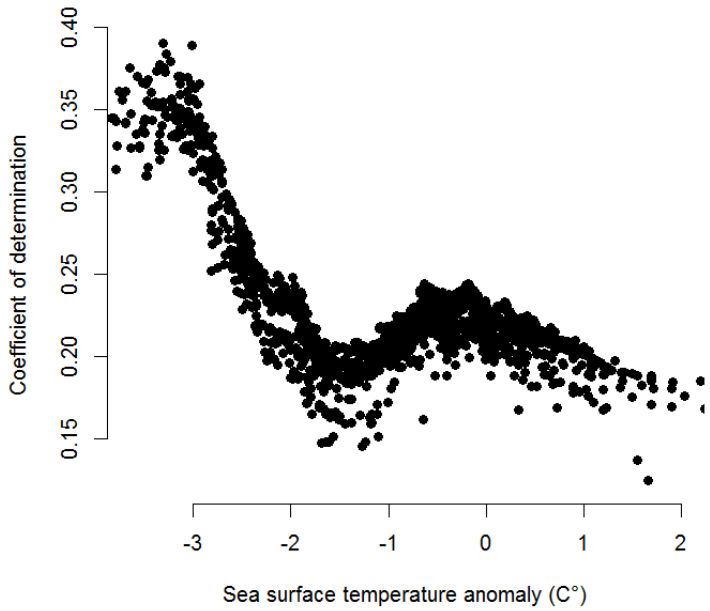

Fig. S5 – Relationship between the SST anomaly (average difference between core inferred SST and SST from 1948-1968 climate across the cores) and the coefficient of determination (R^2) of the bivariate regression between reef fish richness and past coral reef area for each time step of 1000 year (R^2=0.45; lin.=-0.45 quad.=0.49, $P < 0.0001$). R^2 is highest for time periods characterized by overall colder SST. Statistics are provided in the main text.

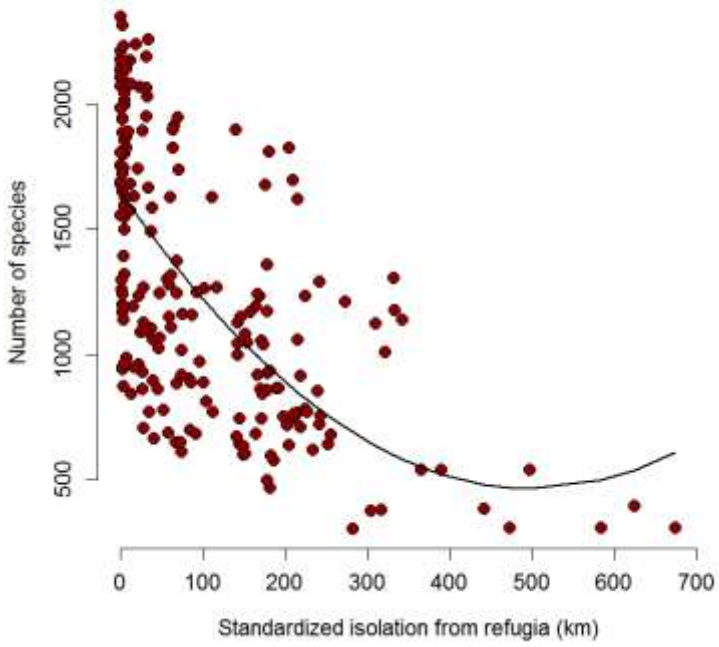

Fig. S6 – Relationship between isolation from refugia and reef fish richness for the Indo-Pacific region. The relationship between isolation from stable areas and fish richness is maintained when the most stable region, the Indo-Pacific, is considered only. Statistics are provided in Table S3.

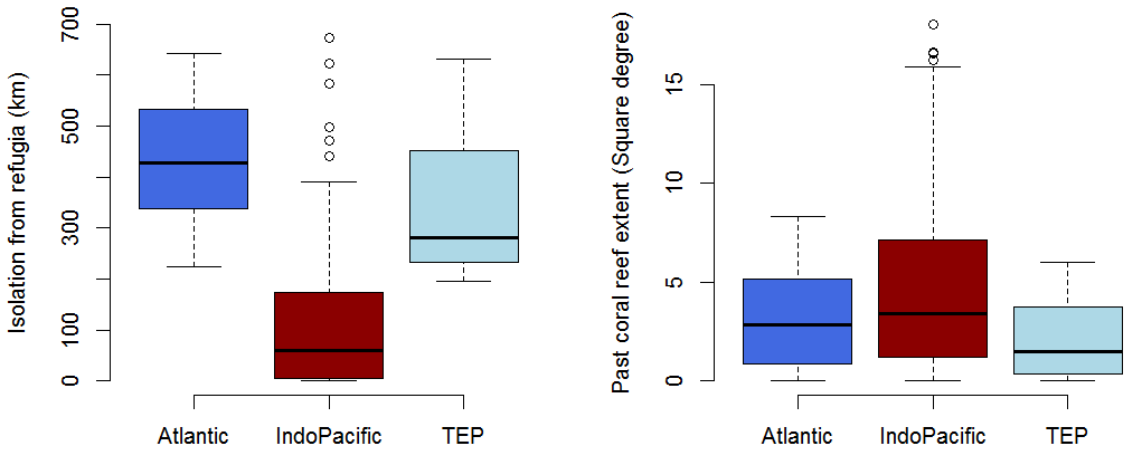

Fig. S7 – Boxplot of past coral reef area (average of the 10th percentile of time steps with coldest sea surface temperature) and isolation from refugia across the three main basins, Atlantic, Indo-Pacific and TEP. Cells located in the Atlantic and TEP basins display smallest coral reef areas during the Quaternary and greater isolation from refugia than those located the Indo-Pacific basin.

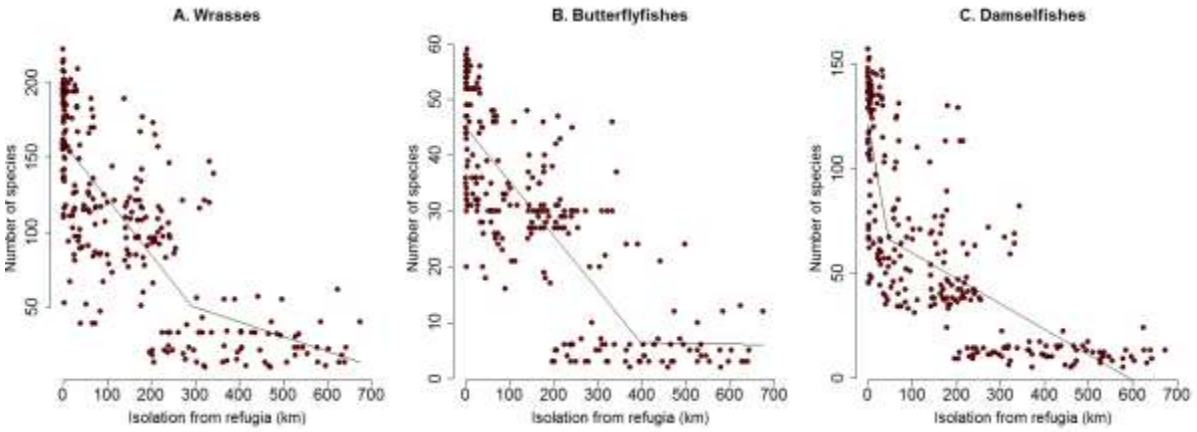

Fig. S8 – Segmented regressions with significant breaking points (P<0.0001) linking the average level of isolation from stable coral reef areas across the Quaternary and richness of reef fishes for three families: Labridae (A), Chaetodontidae (B) and Pomacentridae (C).

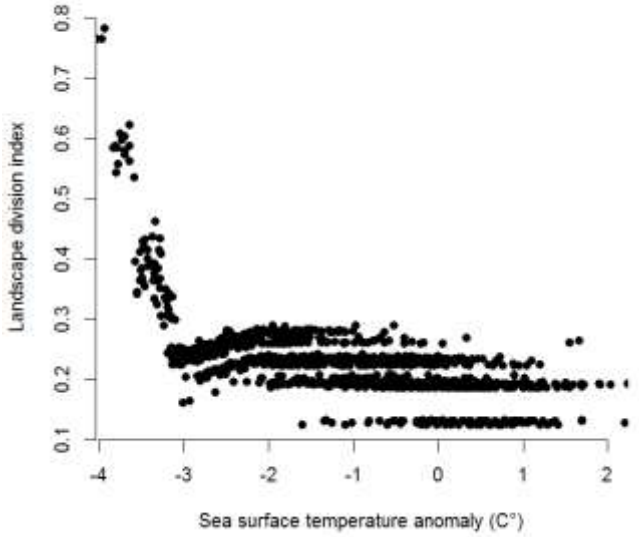

Fig. S9 – Relationship between SST anomaly (average difference between past and current SST across the cores) and fragmentation of coral reef habitat. Fragmentation in the Indo-Pacific basin was highest during the coldest SST and lowest sea level stand. Statistics are provided in the main text.

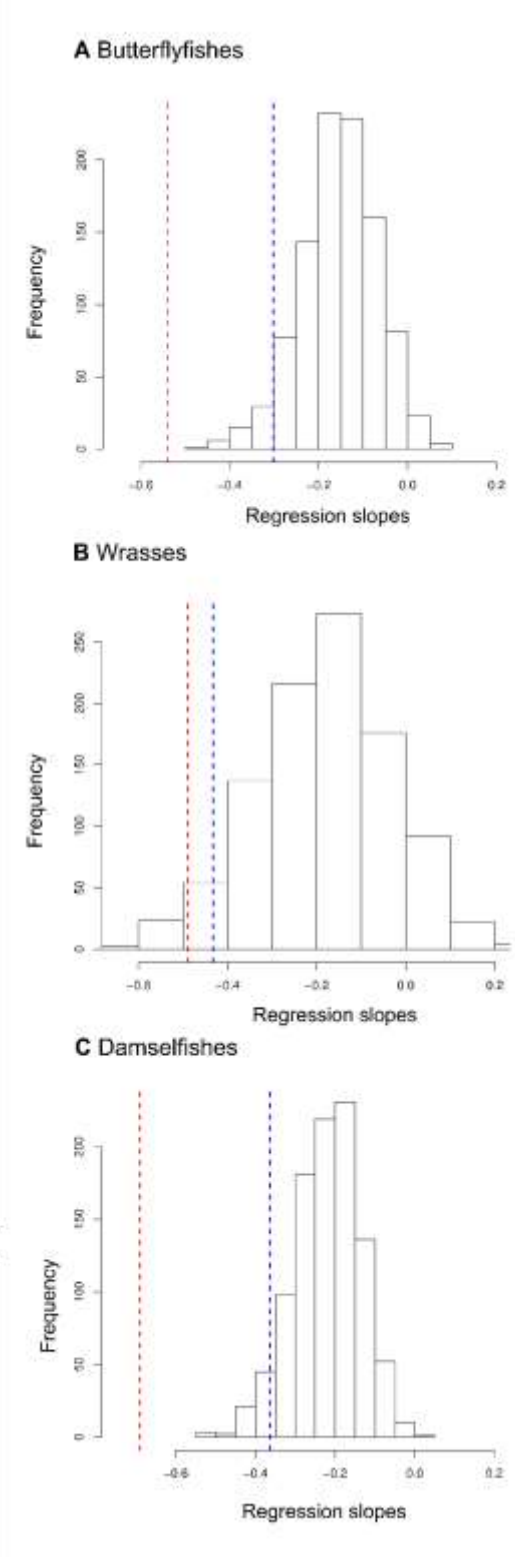

Fig. S10 – Histograms of the standardized regression coefficients estimated from simultaneous autoregressive models (SAR) assessing the relationship between the age range (95^{th}-5^{th} percentile) and isolation from stable areas once the association between species and age was randomized. The blue line indicates the 5^{th} percentile of the distribution and the red line the observed slope.

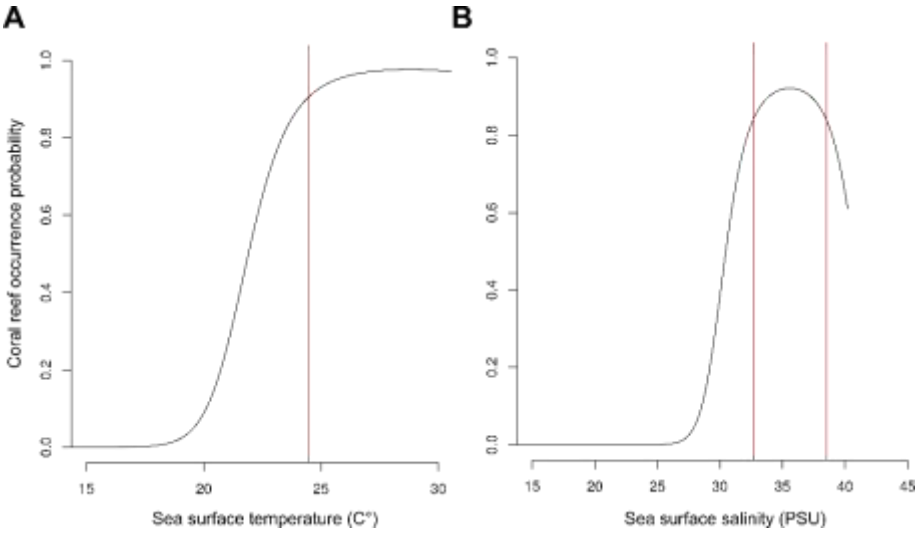

Fig. S11 – (A) Response curve of the coral reef distribution model based on occurrence from www.reefbase.org and average sea surface temperature. As previously documented (6), the optimum of coral reef environmental envelope occurs above of a sea surface temperature threshold of 25°C. Also shown is the response curve in relation to sea surface salinity (B).

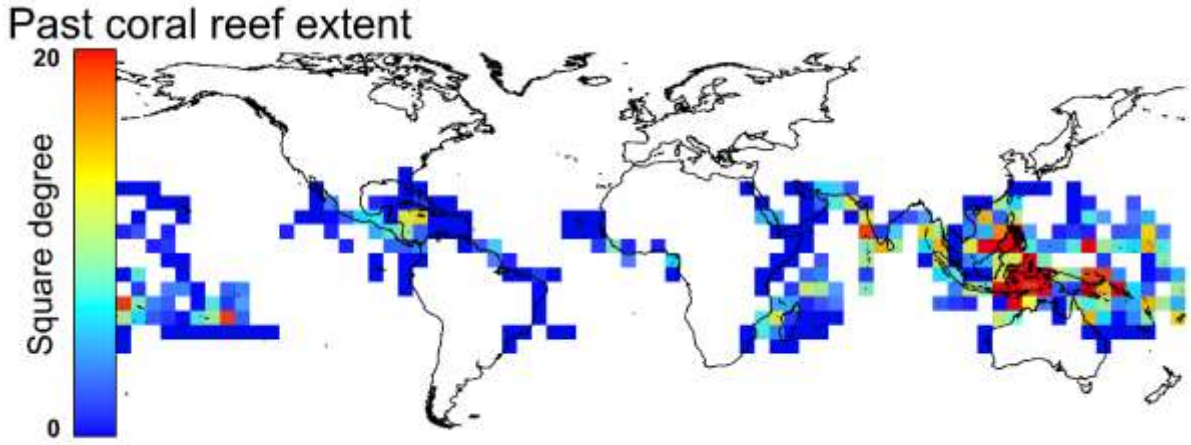

Fig. S12 – Maps of the coral reef area per 5°x5° cell averaged for the periods of marked coral reef contraction, as characterized by lower sea surface temperature and sea level (square degree). This model includes the sea surface temperature anomalies of Annan and Hargreaves (61) and the sea surface salinity reconstruction of Paul and Schäfer-Neth (62). Isolation from coral reef refugia computed from this reconstruction at the last glacial maximum showed a lower explanatory power (R^2=0.18) compared to the index of isolation computed across the Quaternary.

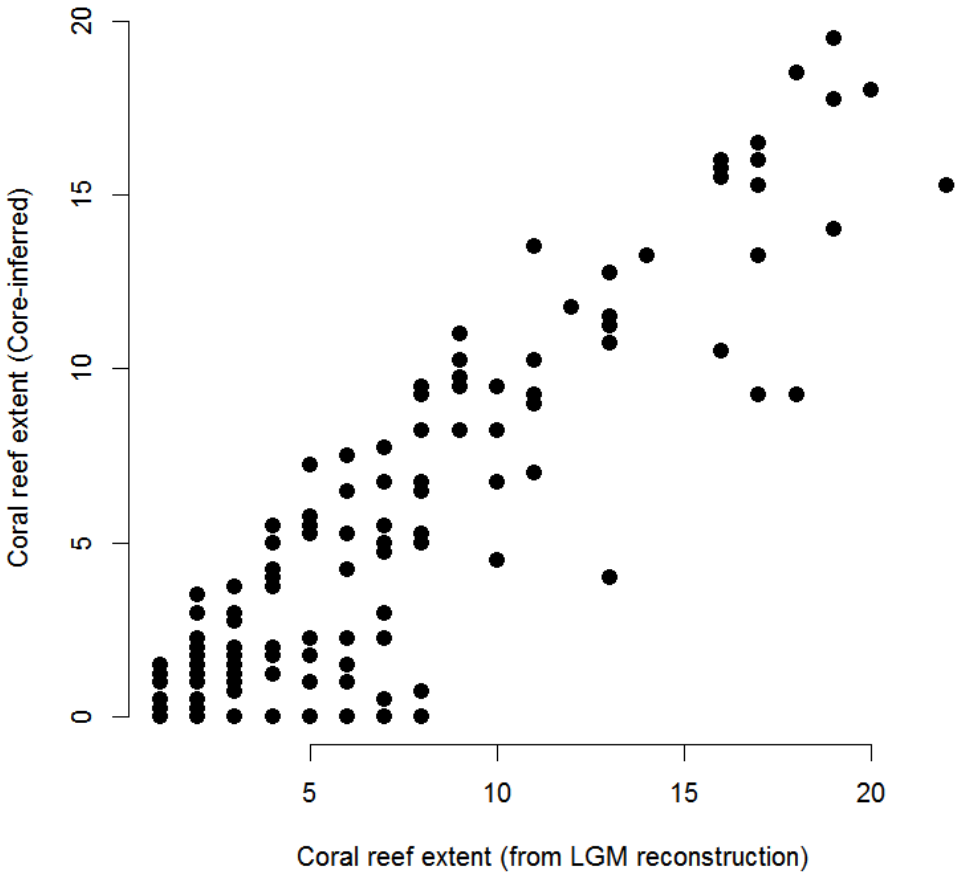

Fig. S13 – Relationship between the extent of coral reef habitat per cell of 5°x5° (square degree) from the sea surface temperature anomalies of Annan and Hargreaves (61) and the sea surface salinity reconstruction of Paul and Schäfer-Neth (62) on x axis and the extent of coral reef inferred from sediment cores and averaged for the period -19 to -23 Ky on y axis. The two reconstructions of the extent of coral reef habitat for the last glacial maximum show good agreement (Pearson's correlation=0.9).

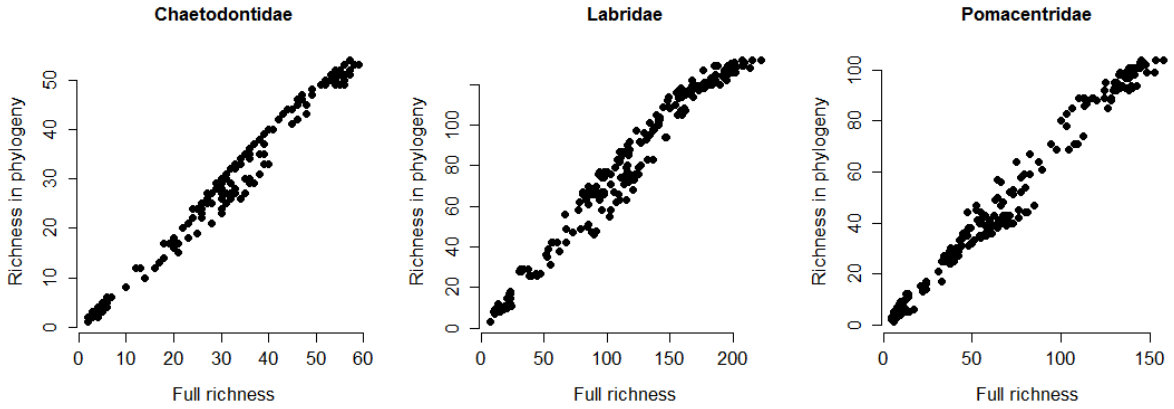

Fig. S14 – Relationship between the richness of taxa contained in the three family phylogenetic trees and the full richness for the three families, Labridae (R^2=97), Chaetodontidae (R^2=0.99) and Pomacentridae (R^2=98). The taxa sampled in the phylogeny are representative of the total richness of assemblage per cell.

Table S1 – Bivariate relationships of five predictor variables to total reef fish richness. PRAR, past coral reef area; PISO, isolation from refugia during the Quaternary; RAR, current coral reef area (log-transformed); ISO, current isolation among coral reef cells, TEMP, average Sea Surface Temperature. Shown are the coefficients of determination (R^2) and the standardized regression coefficients calculated from bivariate ordinary least squares multiple regression (OLS). A SAR model was also used to estimate the standardized coefficients and their statistical significance after having accounted for the effect of spatial autocorrelation. *P < 0.05, **P < 0.01, ***P < 0.001.

		OLS		SAR	
	R^2	Linear	Quadratic	Linear	Quadratic
Historical variables					
PRAR	0.32	0.768 ***	-0.211	0.221 ***	- 0.134 *
PISO	0.62	-1.502 ***	0.803 ***	- 0.576 ***	0.305 ***
Contemporary variables					
RAR	0.33	0.577 ***		0.100 ***	
ISO	0.30	-1.451 ***	1.023 ***	- 0.479 ***	0.269
TEMP	0.25	-5.205 ***	5.664 ***	0.807	- 0.684

Table S2 - Relationships between five predictive factors and total fish richness on coral reefs. PRAR (past coral reef area, log-transformed); PISO (past isolation from refugia during the Quaternary); RAR (current coral reef area, log transformed); ISO (current isolation among coral reef cells). The table shows the coefficient of determination (R^2) and the standardized regression coefficients estimated from ordinary least squares multiple regression (OLS) including all predictor variables (Full model). A simultaneous autoregressive (SAR) model was also used to estimate the standardized coefficients and their statistical significance after having accounted for the effect of spatial autocorrelation. As shown by the Moran's I global, spatial autocorrelation in model residuals was significantly removed in the SAR model. The results of the minimum adequate model (MAM) with the lowest AIC score are also shown for both the OLS and SAR models. The relative importance of each predictor variable was assessed using the summed Akaike weights (W_{AIC}). *P < 0.05, **P < 0.01, ***P < 0.001.

	OLS			SAR		
	Full model	MAM*	W_{AIC}	Full model	MAM	W_{AIC}
Historical variables						
PRAR	-0.106		0.83	0.044		0.46
$PRAR^2$	-0.176		0.49	-0.014		0.16
PISO	-1.077 ***		1	-0.283 *	-0.362 **	0.89
$PISO^2$	0.523 ***		1	0.153	0.209 *	0.66
Contemporary variables						
RAR	0.235 ***		1	0.060 *	0.071 **	0.95
ISO	-0.697 ***		1	-0.309	-0.223 ***	1
ISO^2	0.545 ***		1	0.129		0.32
TEMP	-2.989 **		1	-0.042		0.51
$TEMP^2$	2.888 **		0.98	0.077		0.13
AIC	423.97			158.05	151.23	
R^2	0.738 ***					
Moran's I	0.555 ***			-0.070	-0.065	

* indicates that the full OLS model shows the lowest AIC.

Table S3 - Relationships of five predictor variables to reef fish richness for the Indo-Pacific region only. PRAR (past coral reef area, log-transformed); PISO (past isolation from refugia during the Quaternary); RAR (current coral reef area, log transformed); ISO (current isolation among coral reef cells). The table shows the coefficient of determination (R^2) and the standardized regression coefficients estimated from ordinary least squares multiple regression (OLS) including all predictor variables (Full model). A simultaneous autoregressive (SAR) model was also used to estimate the standardized coefficients and their statistical significance after having accounted for the effect of spatial autocorrelation. As shown by the Moran's I global, spatial autocorrelation in model residuals was significantly removed in the SAR model. The results of the minimum adequate model (MAM) with the lowest AIC score are also shown for both the OLS and SAR models. The relative importance of each predictor variable was assessed using the summed Akaike weights (W_{AIC}). *P < 0.05, **P < 0.01, ***P < 0.001.

	OLS			SAR		
	Full model	MAM	W_{AIC}	Full model	MAM	W_{AIC}
Historical variables						
PRAR	-0.049	0.118	0.78	0.063		0.50
$PRAR^2$	0.145		0.26	- 0.031		0.15
PISO	- 0.576 ***	-0.466 ***	1	-0.175	-0.131 *	0.86
$PISO^2$	0.107		0.38	-0.006		0.29
Contemporary variables						
RAR	0.209 ***	0.202 ***	1	0.073 *	0.083 **	0.89
ISO	-1.125 **	-1.224 **	1	-0.472	-0.251 ***	1
ISO^2	0.794	0.912*	0.81	0.225		0.34
TEMP	-6.518 ***	- 7.174***	1	-1.181		0.38
$TEMP^2$	6.399 ***	7.052 ***	1	1.201		0.15
AIC	401.73	399.175		212.59	204.83	

R^2	0.653 ***	0.639 ***		
Moran's I	0.579 ***	0.582***	-0.057	-0.052

Table S4 - Relationships of five predictor variables to reef fish richness for three families (Labridae, Chaetodontidae and Pomacentridae). PRAR (past coral reef area, log-transformed); PISO (past isolation from refugia during the Quaternary); RAR (current coral reef area, log transformed); ISO (current isolation among coral reef cells). The table shows the coefficient of determination (R^2) and the standardized regression coefficients estimated from ordinary least squares multiple regression (OLS) including all predictor variables (Full model). A simultaneous autoregressive (SAR) model was also used to estimate the standardized coefficients and their statistical significance after having accounted for the effect of spatial autocorrelation. As shown by the Moran's I global, spatial autocorrelation in model residuals was significantly removed in the SAR model. The results of the minimum adequate model (MAM) with the lowest AIC score are also shown for both the OLS and SAR models. The relative importance of each predictor variable was assessed using the summed Akaike weights (W_{AIC}). *P < 0.05, **P < 0.01, ***P < 0.001.

	OLS			SAR		
	Full model	MAM*	W_{AIC}	Full model	MAM	W_{AIC}
Labridae						
Historical variables						
PRAR	-0.297*		0.88	0.012		0.52
$PRAR^2$	0.310**		0.84	0.010		0.14
PISO	-1.047 ***		1	-0.185	-0.246 *	0.54
$PISO^2$	0.420 ***		0.99	0.122	0.166 *	0.34
Contemporary variables						
RAR	0.264 ***		1	0.050 *	0.059 ***	0.92
ISO	-0.520 ***		1	-0.350 *	-0.202 **	1
ISO^2	0.411 **		0.98	0.205		0.45
TEMP	-3.111 ***		0.99	-0.120		0.46
$TEMP^2$	3.030 ***		0.97	0.148		0.13
AIC	441.84			121.63	114.45	
R^2	0.720 ***					
Moran's I	0.573 ***			-0.026	-0.022	
Chaetodontidae						
Historical variables						
PRAR	-0.376**		0.94	-0.032		0.39
$PRAR^2$	0.335 **		0.90	0.040		0.11
PISO	-1.164 ***		1	-0.147	-0.047	0.60

$PISO^2$	0.454 **	1	0.080		0.23
Contemporary variables					
RAR	0.194 ***	1	0.035	0.040 *	0.74
ISO	-0.364 **	0.92	-0.215	-0.176 ***	1
ISO^2	0.287 *	0.78	-0.051		0.28
TEMP	-2.762 **	0.99	0.398	0.041	0.58
$TEMP^2$	3.357 **	0.92	-0.370		0.18
AIC	440.71		75.601	67.59	
R^2	0.721 ***				
Moran's I	0.602 ***		-0.031	-0.035	
Pomacentridae					
Historical variables					
PRAR	-0.165	0.98	0.011	0.044 *	0.87
$PRAR^2$	0.258 *	0.84	0.032		0.24
PISO	-1.191 ***	1	-0.272 *	-0.280 **	0.83
$PISO^2$	0.629 ***	1	0.158 *	0.169 *	0.66
Contemporary variables					
RAR	0.188 ***	1	0.030 *	0.028	0.53
ISO	-0.695 ***	1	-0.230	-0.154 ***	1
ISO^2	0.561 ***	1	-0.098		0.31
TEMP	-3.189 ***	1	-0.244		0.36
$TEMP^2$	3.075 ***	0.98	0.261		0.10
AIC	437.79		104.75	97.97	
R^2	0.724 ***				
Moran's I	0.614 ***		-0.046	-0.047	

* indicates that the full OLS model shows the lowest AIC.

Databases S1 as txt archives: *Supplementary_Data_Pellissier.txt*

References and Notes

1. D. R. Bellwood, T. P. Hughes, Regional-scale assembly rules and biodiversity of coral reefs. *Science* **292**, 1532–1535 (2001). Medline doi:10.1126/science.1058635

2. W. Renema, D. R. Bellwood, J. C. Braga, K. Bromfield, R. Hall, K. G. Johnson, P. Lunt, C. P. Meyer, L. B. McMonagle, R. J. Morley, A. O'Dea, J. A. Todd, F. P. Wesselingh, M. E. Wilson, J. M. Pandolfi, Hopping hotspots: Global shifts in marine biodiversity. *Science* **321**, 654–657 (2008). Medline doi:10.1126/science.1155674

3. S. A. Price, R. Holzman, T. J. Near, P. C. Wainwright, Coral reefs promote the evolution of morphological diversity and ecological novelty in labrid fishes. *Ecol. Lett.* **14**, 462–469 (2011). Medline doi:10.1111/j.1461-0248.2011.01607.x

4. P. F. Cowman, D. R. Bellwood, The historical biogeography of coral reef fishes: Global patterns of origination and dispersal. *J. Biogeogr.* **40**, 209–224 (2013). doi:10.1111/jbi.12003

5. V. Parravicini, M. Kulbicki, D. R. Bellwood, A. M. Friedlander, J. E. Arias-Gonzalez, P. Chabanet, S. R. Floeter, R. Myers, L. Vigliola, S. D'Agata, D. Mouillot, Global patterns and predictors of tropical reef fish species richness. *Ecography* **36**, 1254–1262 (2013). doi:10.1111/j.1600-0587.2013.00291.x

6. J. A. Kleypas *et al*., *Am. Zool.* **39**, 146 (1999).

7. J. H. Connell, T. P. Hughes, C. C. Wallace, A 30-year study of coral abundance, recruitment, and disturbance at several scales in space and time. *Ecol. Monogr.* **67**, 461–488 (1997). doi:10.1890/0012-9615(1997)067[0461:AYSOCA]2.0.CO;2

8. T. P. Hughes, A. H. Baird, E. A. Dinsdale, N. A. Moltschaniwskyj, M. S. Pratchett, J. E. Tanner, B. L. Willis, Assembly rules of reef corals are flexible along a steep climatic gradient. *Curr. Biol.* **22**, 736–741 (2012). Medline doi:10.1016/j.cub.2012.02.068

9. W. Kiessling, C. Simpson, B. Beck, H. Mewis, J. M. Pandolfi, Equatorial decline of reef corals during the last Pleistocene interglacial. *Proc. Natl. Acad. Sci. U.S.A.* **109**, 21378–21383 (2012). Medline doi:10.1073/pnas.1214037110

10. J. E. N. Veron, M. Stafford-Smith, *Corals of the World* (Australian Institute of Marine Science, Townsville, Australia, 2000).

11. M. J. Paddack, J. D. Reynolds, C. Aguilar, R. S. Appeldoorn, J. Beets, E. W. Burkett, P. M. Chittaro, K. Clarke, R. Esteves, A. C. Fonseca, G. E. Forrester, A. M. Friedlander, J. García-Sais, G. González-Sansón, L. K. Jordan, D. B. McClellan, M. W. Miller, P. P. Molloy, P. J. Mumby, I. Nagelkerken, M. Nemeth, R. Navas-Camacho, J. Pitt, N. V. Polunin, M. C. Reyes-Nivia, D. R. Robertson, A. Rodríguez-Ramírez, E. Salas, S. R. Smith, R. E. Spieler, M. A. Steele, I. D. Williams, C. L. Wormald, A. R. Watkinson, I. M. Côté, Recent region-wide declines in Caribbean reef fish abundance. *Curr. Biol.* **19**, 590–595 (2009). Medline doi:10.1016/j.cub.2009.02.041

12. M. C. Bonin, G. R. Almany, G. P. Jones, Contrasting effects of habitat loss and fragmentation on coral-associated reef fishes. *Ecology* **92**, 1503–1512 (2011). Medline doi:10.1890/10-0627.1

13. G. Paulay, *Paleobiology* **16**, 415–434 (1990).

14. A. C. Carnaval, M. J. Hickerson, C. F. Haddad, M. T. Rodrigues, C. Moritz, Stability predicts genetic diversity in the Brazilian Atlantic forest hotspot. *Science* **323**, 785–789 (2009). Medline doi:10.1126/science.1166955

15. B. Sandel, L. Arge, B. Dalsgaard, R. G. Davies, K. J. Gaston, W. J. Sutherland, J. C. Svenning, The influence of Late Quaternary climate-change velocity on species endemism. *Science* **334**, 660–664 (2011). Medline doi:10.1126/science.1210173

16. D. D. McKenna, B. D. Farrell, Tropical forests are both evolutionary cradles and museums of leaf beetle diversity. *Proc. Natl. Acad. Sci. U.S.A.* **103**, 10947–10951 (2006). Medline doi:10.1073/pnas.0602712103

17. K. G. Miller, M. A. Kominz, J. V. Browning, J. D. Wright, G. S. Mountain, M. E. Katz, P. J. Sugarman, B. S. Cramer, N. Christie-Blick, S. F. Pekar, The Phanerozoic record of global sea-level change. *Science* **310**, 1293–1298 (2005). Medline doi:10.1126/science.1116412

18. T. D. Herbert, L. C. Peterson, K. T. Lawrence, Z. Liu, Tropical ocean temperatures over the past 3.5 million years. *Science* **328**, 1530–1534 (2010). Medline doi:10.1126/science.1185435

19. M. L. Rosenzweig, *Species Diversity in Space and Time* (Cambridge Univ. Press, Cambridge, 1995).

20. S. L. Chown, K. J. Gaston, Areas, cradles and museums: The latitudinal gradient in species richness. *Trends Ecol. Evol.* **15**, 311–315 (2000). Medline doi:10.1016/S0169-5347(00)01910-8

21. O. J. Luiz, A. P. Allen, D. R. Robertson, S. R. Floeter, M. Kulbicki, L. Vigliola, R. Becheler, J. S. Madin, Adult and larval traits as determinants of geographic range size among tropical reef fishes. *Proc. Natl. Acad. Sci. U.S.A.* **110**, 16498–16502 (2013). Medline doi:10.1073/pnas.1304074110

22. J. W. McManus, "Marine speciation, tectonics, and sea-level changes in Southeast Asia," in *Proceedings of the Fifth International Coral Reef Congress*, C. Gabrie, B. Salvat, Eds. (International Coral Reef Symposium, Penang, Malaysia, 1985), vol. **4**, pp. 133–138.

23. D. C. Potts, "Sea-level fluctuations and speciation in scleractinia," in *Proceedings of the Fifth International Coral Reef Congress*, C. Gabrie, B. Salvat, Eds. (International Coral Reef Symposium, Penang, Malaysia, 1985), vol. 4, pp. 127–132.

24. A. J. Kohn, "Evolutionary ecology of Consu on Indo-Pacific coral reefs," in *Proceedings of the Fifth International Coral Reef Congress*, C. Gabrie, B. Salvat, Eds. (International Coral Reef Symposium, Penang, Malaysia, 1995) vol. 4, pp. 139–144.

25. J. Fjeldså, J. C. Lovett, *Biodivers. Conserv.* **6**, 325–346 (1997). doi:10.1023/A:1018356506390

26. C. Mora, P. M. Chittaro, P. F. Sale, J. P. Kritzer, S. A. Ludsin, Patterns and processes in reef fish diversity. *Nature* **421**, 933–936 (2003). Medline doi:10.1038/nature01393

27. P. H. Barber, D. R. Bellwood, Biodiversity hotspots: evolutionary origins of biodiversity in wrasses (Halichoeres: Labridae) in the Indo-Pacific and new world tropics. *Mol. Phylogenetics Evol.* **35**, 235–253 (2005). doi:10.1016/j.ympev.2004.10.004

28. D. R. Bellwood, C. P. Meyer, Searching for heat in a marine biodiversity hotspot. *J. Biogeogr.* **36**, 569–576 (2009). doi:10.1111/j.1365-2699.2008.02029.x

29. D. R. Bellwood, P. C. Wainwright, in *Coral Reef Fishes: Dynamics and Diversity in a Complex Ecosystem*, P. F. Sale, Ed. (Academic Press, San Diego, CA, 2002).

30. A. O'Dea, J. B. Jackson, H. Fortunato, J. T. Smith, L. D'Croz, K. G. Johnson, J. A. Todd, Environmental change preceded Caribbean extinction by 2 million years. *Proc. Natl. Acad. Sci. U.S.A.* **104**, 5501–5506 (2007). Medline doi:10.1073/pnas.0610947104

31. C. H. Graham, C. Moritz, S. E. Williams, Habitat history improves prediction of biodiversity in rainforest fauna. *Proc. Natl. Acad. Sci. U.S.A.* **103**, 632–636 (2006). Medline doi:10.1073/pnas.0505754103

32. J. M. Pandolfi, S. R. Connolly, D. J. Marshall, A. L. Cohen, Projecting coral reef futures under global warming and ocean acidification. *Science* **333**, 418–422 (2011). Medline doi:10.1126/science.1204794

33. C. Mora, C. L. Wei, A. Rollo, T. Amaro, A. R. Baco, D. Billett, L. Bopp, Q. Chen, M. Collier, R. Danovaro, A. J. Gooday, B. M. Grupe, P. R. Halloran, J. Ingels, D. O. Jones, L. A. Levin, H. Nakano, K. Norling, E. Ramirez-Llodra, M. Rex, H. A. Ruhl, C. R. Smith, A. K. Sweetman, A. R. Thurber, J. F. Tjiputra, P. Usseglio, L. Watling, T. Wu, M. Yasuhara, Biotic and human vulnerability to projected changes in ocean biogeochemistry over the 21st century. *PLOS Biol.* **11**, e1001682 (2013). Medline doi:10.1371/journal.pbio.1001682

34. A. Sterl, R. Bintanja, L. Brodeau, E. Gleeson, T. Koenigk, T. Schmith, T. Semmler, C. Severijns, K. Wyser, S. Yang, A look at the ocean in the EC-Earth climate model. *Clim. Dyn.* **39**, 2631–2657 (2012). doi:10.1007/s00382-011-1239-2

35. E. Kalnay, M. Kanamitsu, R. Kistler, W. Collins, D. Deaven, L. Gandin, M. Iredell, S. Saha, G. White, J. Woollen, Y. Zhu, A. Leetmaa, R. Reynolds, M. Chelliah, W. Ebisuzaki, W. Higgins, J. Janowiak, K. C. Mo, C. Ropelewski, J. Wang, R. Jenne, D. Joseph, The NCEP/NCAR 40-Year Reanalysis Project. *Bull. Am. Meteorol. Soc.* **77**, 437–471 (1996). doi:10.1175/1520-0477(1996)077<0437:TNYRP>2.0.CO;2

36. D. Nürnberg, A. Müller, R. R. Schneider, Paleo-sea surface temperature calculations in the equatorial east Atlantic from Mg/Ca ratios in planktic foraminifera: A comparison to sea surface temperature estimates from $U_{37}^{K'}$, oxygen isotopes, and foraminiferal transfer function. *Paleoceanography* **15**, 124–134 (2000). doi:10.1029/1999PA000370

37. E. L. Sikes, L. D. Keigwin, Equatorial Atlantic sea surface temperature for the last 30 kyr: A comparison of $U_{37}^{k'}$, $\delta^{18}O$ and foraminiferal assemblage temperature estimates. *Paleoceanography* **9**, 31–45 (1994). doi:10.1029/93PA02198

38. M. Zhao, N. A. S. Beveridge, N. J. Shackleton, M. Sarnthein, G. Eglinton, Molecular stratigraphy of cores off northwest Africa: Sea surface temperature history over the last 80 Ka. *Paleoceanography* **10**, 661–675 (1995). doi:10.1029/94PA03354

39. Y. Rosenthal *et al*., The amplitude and phasing of climate change during the last deglaciation in the Sulu Sea, western equatorial Pacific. *Geophys. Res. Lett.* **30**, 1428 (2003). doi:10.1029/2002GL016612

40. R. R. Schneider, P. J. Müller, G. Ruhland, Late Quaternary surface circulation in the east equatorial South Atlantic: Evidence from Alkenone sea surface temperatures. *Paleoceanography* **10**, 197–219 (1995). doi:10.1029/94PA03308

41. E. L. McClymont, A. Rosell-Mele, Links between the onset of modern Walker circulation and the mid-Pleistocene climate transition. *Geology* **33**, 389 (2005). doi:10.1130/G21292.1

42. M. W. Schmidt, H. J. Spero, D. W. Lea, Links between salinity variation in the Caribbean and North Atlantic thermohaline circulation. *Nature* **428**, 160–163 (2004). Medline doi:10.1038/nature02346

43. E. C. Farmer, P. B. deMenocal, T. M. Marchitto, Holocene and deglacial ocean temperature variability in the Benguela upwelling region: Implications for low-latitude atmospheric circulation. *Paleoceanography* **20**, PA2018 (2005). doi:10.1029/2004PA001049

44. D. W. Lea, D. K. Pak, L. C. Peterson, K. A. Hughen, Synchroneity of tropical and high-latitude Atlantic temperatures over the last glacial termination. *Science* **301**, 1361–1364 (2003). Medline doi:10.1126/science.1088470

45. D. W. Lea, D. K. Pak, H. J. Spero, Climate impact of late quaternary equatorial pacific sea surface temperature variations. *Science* **289**, 1719–1724 (2000). Medline doi:10.1126/science.289.5485.1719

46. M. Kienast, S. Steinke, K. Stattegger, S. E. Calvert, Synchronous tropical South China Sea SST change and Greenland warming during deglaciation. *Science* **291**, 2132–2134 (2001). Medline doi:10.1126/science.1057131

47. S. S. Kienast, J. L. McKay, Sea surface temperatures in the subarctic northeast Pacific reflect millennial-scale climate oscillations during the last 16 kyrs. *Geophys. Res. Lett.* **28**, 1563–1566 (2001). doi:10.1029/2000GL012543

48. L. Stott, K. Cannariato, R. Thunell, G. H. Haug, A. Koutavas, S. Lund, Decline of surface temperature and salinity in the western tropical Pacific Ocean in the Holocene epoch. *Nature* **431**, 56–59 (2004). Medline doi:10.1038/nature02903

49. L. Li, Q. Li, J. Tian, P. Wang, H. Wang, Z. Liu, A 4-Ma record of thermal evolution in the tropical western Pacific and its implications on climate change. *Earth Planet. Sci. Lett.* **309**, 10–20 (2011). doi:10.1016/j.epsl.2011.04.016

50. J. P. LaRiviere, A. C. Ravelo, A. Crimmins, P. S. Dekens, H. L. Ford, M. Lyle, M. W. Wara, Late Miocene decoupling of oceanic warmth and atmospheric carbon dioxide forcing. *Nature* **486**, 97–100 (2012). Medline doi:10.1038/nature11200

51. S. L. Coles, P. L. Jokiel, Effects of temperature on photosynthesis and respiration in hermatypic corals. *Mar. Biol.* **43**, 209–216 (1977). doi:10.1007/BF00402313

52. A. T. Marshall, P. Clode, *Coral Reefs* **23**, 218 (2004).

53. S. L. Coles, Y. H. Fadlallah, Reef coral survival and mortality at low temperatures in the Arabian Gulf: New species-specific lower temperature limits. *Coral Reefs* **9**, 231–237 (1991). doi:10.1007/BF00290427

54. A. Guisan, N. E. Zimmermann, Predictive habitat distribution models in ecology. *Ecol. Modell.* **135**, 147–186 (2000). doi:10.1016/S0304-3800(00)00354-9

55. M. S. Wisz, A. Guisan, Do pseudo-absence selection strategies influence species distribution models and their predictions? An information-theoretic approach based on simulated data. *BMC Ecol.* **9**, 8 (2009). Medline doi:10.1186/1472-6785-9-8

56. P. W. Glynn, L. D'Croz, Experimental evidence for high temperature stress as the cause of El Niño-coincident coral mortality. *Coral Reefs* **8**, 181–191 (1990). doi:10.1007/BF00265009

57. P. L. Munday, M. J. Kingsford, M. O'Callaghan, J. M. Donelson, Elevated temperature restricts growth potential of the coral reef fish Acanthochromis polyacanthus. *Coral Reefs* **27**, 927–931 (2008). doi:10.1007/s00338-008-0393-4

58. L. T. Toth, R. B. Aronson, S. V. Vollmer, J. W. Hobbs, D. H. Urrego, H. Cheng, I. C. Enochs, D. J. Combosch, R. van Woesik, I. G. Macintyre, ENSO drove 2500-year collapse of Eastern Pacific coral reefs. *Science* **337**, 81–84 (2012). doi:10.1126/science.1221168

59. C. Liu, P. M. Berry, T. P. Dawson, R. G. Pearson, Selecting thresholds of occurrence in the prediction of species distributions. *Ecography* **28**, 385–393 (2005). doi:10.1111/j.0906-7590.2005.03957.x

60. D. P. Tittensor, A. R. Baco, P. E. Brewin, M. R. Clark, M. Consalvey, J. Hall-Spencer, A. A. Rowden, T. Schlacher, K. I. Stocks, A. D. Rogers, Predicting global habitat suitability for stony corals on seamounts. *J. Biogeogr.* **36**, 1111–1128 (2009). doi:10.1111/j.1365-2699.2008.02062.x

61. J. D. Annan, J. C. Hargreaves, A new global reconstruction of temperature changes at the Last Glacial Maximum. *Clim. Past* **9**, 367–376 (2013). doi:10.5194/cp-9-367-2013

62. A. Paul, C. Schäfer-Neth, Modeling the water masses of the Atlantic Ocean at the Last Glacial Maximum. *Paleoceanography* **18**, 1058 (2003). doi:10.1029/2002PA000783

63. R. van Etten, *Technical report, gdistance vignette* (2012).

64. R Development Core Team, www.R-project.org.

65. J. VanDerWal, L. *Technical report, SDMTools vignette* (2013).

66. M. D. Spalding, H. E. Fox, G. R. Allen, N. Davidson, Z. A. Ferdaña, M. Finlayson, B. S. Halpern, M. A. Jorge, A. L. Lombana, S. A. Lourie, K. D. Martin, E. McManus, J. Molnar, C. A. Recchia, J. Robertson, Marine ecoregions of the World: A bioregionalization of coastal and shelf areas. *Bioscience* **57**, 573 (2007). doi:10.1641/B570707

67. L. B. Buckley, W. Jetz, Environmental and historical constraints on global patterns of amphibian richness. *Proc. R. Soc. London Ser. B* **274**, 1167–1173 (2007). doi:10.1098/rspb.2006.0436

68. S. Andréfouët *et al*., "Global assessment of modern coral reef extent and diversity for regional science and management applications: A view from space," in *Proceedings of 10th International Coral Reef Symposium* (International Coral Reef Symposium, Penang, Malaysia, 2006), pp. 1732–1745.

69. D. R. Bellwood, T. P. Hughes, S. R. Connolly, J. Tanner, Environmental and geometric constraints on Indo-Pacific coral reef biodiversity. *Ecol. Lett.* **8**, 643–651 (2005). doi:10.1111/j.1461-0248.2005.00763.x

70. A. Moilanen, M. Nieminen, Simple connectivity measures in spatial ecology. *Ecology* **83**, 1131–1145 (2002). doi:10.1890/0012-9658(2002)083[1131:SCMISE]2.0.CO;2

71. D. J. Currie, Energy and large-scale patterns of animal- and plant-species richness. *Am. Nat.* **137**, 27 (1991). doi:10.1086/285144

72. D. P. Tittensor, C. Mora, W. Jetz, H. K. Lotze, D. Ricard, E. V. Berghe, B. Worm, Global patterns and predictors of marine biodiversity across taxa. *Nature* **466**, 1098–1101 (2010). Medline doi:10.1038/nature09329

73. C. F. Dormann *et al*., J. M. McPherson, M. B. Araújo, R. Bivand, J. Bolliger, G. Carl, R. G. Davies, A. Hirzel, W. Jetz, W. Daniel Kissling, I. Kühn, R. Ohlemüller, P. R. Peres-Neto, B. Reineking, B. Schröder, F. M. Schurr, R. Wilson, Methods to account for spatial autocorrelation in the analysis of species distributional data: A review. *Ecography* **30**, 609 (2007). doi:10.1111/j.2007.0906-7590.05171.x

74. W. D. Kissling, R. Field, K. Böhning-Gaese, Spatial patterns of woody plant and bird diversity: Functional relationships or environmental effects? *Glob. Ecol. Biogeogr.* **17**, 59 (2008). doi:10.1111/j.1466-8238.2007.00379.x

75. K. P. Burnham, D. R. Anderson, *Model Selection and Multimodel Inference: A Practical Information-Theoretic Approach* (Springer-Verlag, Berlin, ed. 2, 2002).

76. J. A. F. Diniz-Filho, T. F. L. V. B. Rangel, L. M. Bini, Model selection and information theory in geographical ecology. *Glob. Ecol. Biogeogr.* **17**, 479–488 (2008). doi:10.1111/j.1466-8238.2008.00395.x

77. K. Bartoń, *Technical report, MuMIn vignette* (2009).

78. D. Borcard, P. Legendre, P. Drapeau, Partialling out the spatial component of ecological variation. *Ecology* **73**, 1045 (1992). doi:10.2307/1940179

79. P. Legendre, L. Legendre, *Numerical Ecology* (Elsevier, Amsterdam, 2012).

80. V. M. Muggeo, *R News* **8**, 20 (2008).